Geochemical Journal, Vol. 52, pp. 457 to 466, 2018 doi:10.2343/geochemj.2.0534

# Hydrogen isotope analysis of micro-scale apatite inclusions in Archaean zircon grains

Akizumi Ishida,[1]* Mizuho Koike,[1] Naoto Takahata,[1] Takuya Morita,[1] Jean David,[2,3] Daniele L. Pinti[2] and Yuji Sano[1]

[1]Atmosphere and Ocean Research Institute, The University of Tokyo, 5-1-5 Kashiwanoha, Kashiwa, Chiba 277-8564, Japan
[2]GEOTOP, Research Center for the Dynamics of the Earth System, Université du Québec à Montréal, CP. 8888 Centre-Ville, H3C3P8, QC, Canada
[3]Bureau d'Exploration Géologique du Québec, Ministère de l'Énergie et des Ressources Naturelles, Université du Québec à Montréal, Succ. Centre-Ville, Montréal, Québec H3C3P8, Canada

(*Received December 20, 2017; Accepted July 27, 2018*)

A novel study of *in situ* hydrogen isotope composition ($\delta$D) measurements of micron-scale apatite inclusions hosted in zircon crystals was carried out by lateral high-resolution secondary ion mass spectrometry. The host rock of zircon is a tonalite belonging to the Nuvvuagittuq Supracrustal belt, Canada, which is considered to be one of the oldest supracrustal belts of Hadean-Archean age. Uranium-lead dating of host zircon crystals yielded an age of 3636 ± 20 Ma, which is consistent with previously reported ages of this unit. The $\delta$D values were measured for seven apatite inclusions, and range from –225 to +65‰ (vs. SMOW). A negative correlation was observed between $\delta$D values and the $^{18}O^-/^1H^-$ ratios of the examined apatite inclusions. This relationship can be explained by a mixing trend between the original hydrogen in the apatite inclusions and contamination from the analytical environment. The pristine $\delta$D value estimated for the apatite inclusion is +53 ± 60‰, which was clearly distinct from the $\delta$D value resulting from bulk rock analysis, –49 ± 2‰. The pristine $\delta$D value of the tonalitic magma source may provide new constraints on the formation of the primitive crust and/or the ocean of the early Earth.

Keywords: NanoSIMS, hydrogen isotope composition, U-Pb dating, Archean, apatite inclusion

## Introduction

Hydrogen isotope compositions (i.e., deuterium/hydrogen; (D/H) ratio) of terrestrial reservoirs (e.g., mantle, crust, and ocean water) inform our understanding of the origin and evolution of water on Earth. Studies focused on subduction zones provide important insight into the recycling of surface water into the mantle (e.g., Stern *et al*., 2003; Wallace, 2005; Shaw *et al*., 2008). Several studies have been carried out to understand water cycling through a subduction zone, targeting D/H ratios of volcanic fumaroles, submarine basalts, and hydrous minerals or inclusions (e.g., Allard, 1983; Giggenbach, 1992; Stolper and Newman, 1994; Miyagi and Matsubaya, 2003; Shaw *et al*., 2008). However, measured values may be affected by metamorphism and/or contamination by modern seawater, which masks the original isotopic compositions. Co-evolution processes between surface and interior water throughout geological history remain controversial.

Evidence of an Archean subduction setting are recognized in Isua, Greenland and Labrador, Canada, the ages of which are estimated to be *ca*. 3.7 Ga (Nutman *et al*., 1997; Polat *et al*., 2002; Jenner *et al*., 2009; Komiya *et al*., 2015). These terrains consist of ordered layers of serpentinized oceanic crust, pillow lavas, schists, and banded iron formations (BIFs), suggesting that continental accretion driven by same sort of subduction mechanism, already existed at that time (e.g., Furnes *et al*., 2007; Arai *et al*., 2015). It is inferred that the transportation of water from the surface to the interior had begun by *ca*. 3.7 Ga (e.g., Cawood *et al*., 2013; Yuan, 2015; Tang *et al*., 2016).

Turner *et al*. (2014) suggested that the Nuvvuagittuq Greenstone Belt (NGB), one of Earth's oldest primitive crusts, located in northern Québec (Canada), could represent a subduction zone. This is based on similarities of the local stratigraphy and rock geochemistry with those of the modern Izu-Bonin-Mariana forearc (Turner *et al*., 2014). NGB units include tonalitic gneiss, gabbro, amphibolite, and BIFs, together with felsic units, which might be metamorphosed sediments (David *et al*., 2009; O'Neil *et al*., 2011). All these units were metamorphosed

*Corresponding author (e-mail: ishidaz@tohoku.ac.jp)
*Present address: Institute for Excellence in Higher Education, Tohoku University, 6-3 Aramaki Aza Aoba, Aobaku, Sendai 980-8576, Japan.

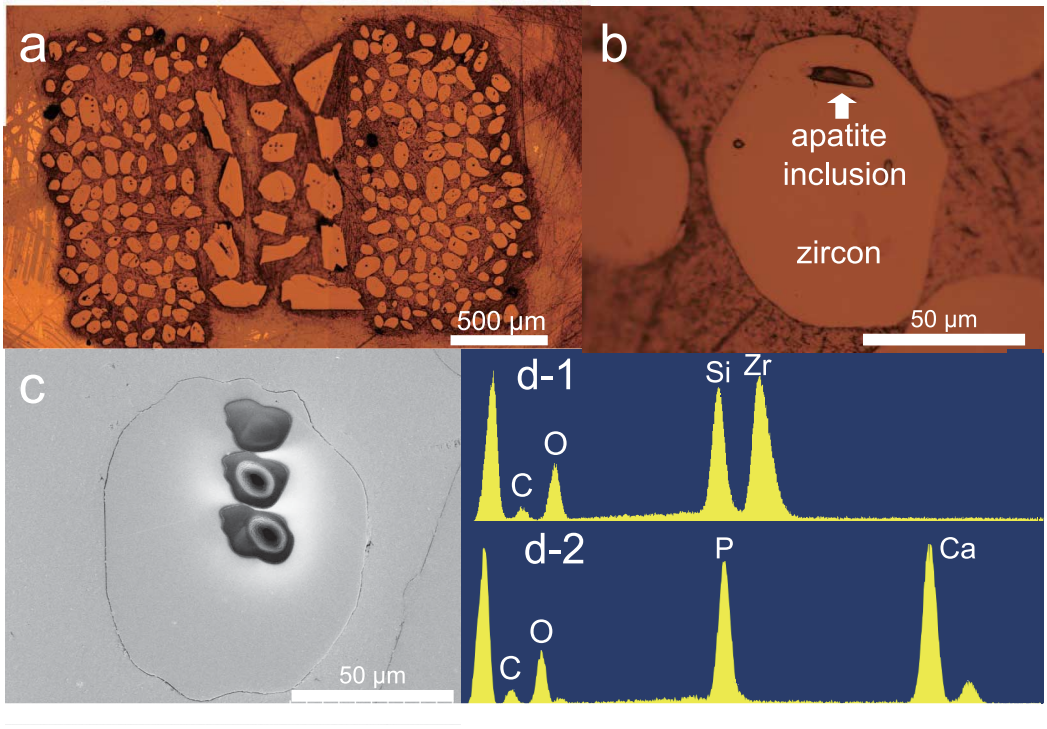


*Fig. 1. a: Examined zircon grains mounted in resin (smaller grains), and reference zircon grains (larger grains). b: Typical apatite inclusion found in zircon grain. c: Zircon grain and analytical spot for U-Pb dating session. d: Chemical compositions of zircon (d-1) and apatite inclusion (d-2), determined by EDX.*

up to granulite facies, as generally found in the neighboring Minto block (Percival *et al.*, 1992). Conversely, some previous datasets suggest that subduction did not begin until 3 Ga (e.g., Stern, 2005; Dhuime *et al.*, 2012). In such models, the primitive crust might be formed by the partial melting of oceanic plateaus or tectonically thickened island arc crust without requiring a subduction setting (e.g., Nutman *et al.*, 1999; Smithies, 2000; Condie, 2005).

The age of the Nuvvuagittuq geological section was estimated to 4.28 Ga, based on the correlation between $^{142}Nd/^{144}Nd$ and $^{147}Sm/^{144}Nd$ measured in amphibolite rocks (O'Neil *et al.*, 2008). This age was subsequently contested, because of the spurious correlation between rocks that were possibly not co-genetic (Andreasen and Sharma, 2009). U-Pb zircon dating from the same unit shows a lower maximum age, of 3.83 Ga (Cates and Mojzsis, 2007; O'Neil *et al.*, 2008; David *et al.*, 2009). Although the true formation age of the primitive crust is still debated, the age of the tonalite unit surrounding the crustal unit is estimated to be 3.66 Ga (David *et al.*, 2009).

The D/H ratio of the global ocean at 3.7 Ga is considered to have been lower than that of the modern one. Pope *et al.* (2012) estimated a D/H ratio of the Archean ocean from the ratio of associating serpentine, assuming isotope fractionation between seawater and serpentine under hydrothermal conditions. They concluded that the D/H ratio of the ocean evolved from a lighter value at 3.7 Ga ($\delta D = -25 \pm 5‰$, where $\delta D = [(D/H)_{sample}/(D/H)_{SMOW} - 1] \times 1000$, with reference to Standard Mean Ocean Water (SMOW; $D/H = 1.5576 \times 10^{-4}$)), to a heavier modern value ($\delta D = 0‰$). This D/H evolution could be explained by the preferential loss of $^{1}H$ during hydrogen escape into the space over geological time (Pope *et al.*, 2012). However, such bulk rock analysis can include ambiguous origin of hydrogen which was contaminated or fractionated by the later geological process.

Zircon is one of the most common minerals found in both volcanic and sedimentary rocks. It is known to be a metamorphic-resistant mineral, suggesting that its inclusion minerals may be protected from metamorphism. Incompatible elements with the high field strength elements, such as hafnium, tend to be sealed in zircon (e.g., Patchett *et al.*, 1981; Griffin *et al.*, 2004). On the other hand, apatite, which is one of the most common inclusion crystals found in zircon, tends to contain other incompatible elements, such as hydrogen, strontium, and halogens (e.g., Watson, 1979, 1980; Prowatke and Klemme, 2006). These results suggest that apatite inclusions hosted in zircon should be shielded from metamorphism, and thus may preserve the primitive elemental information of the coexisting magma. By combining U-Pb dating of the host

*Table 1. Summary of U-Pb dating of examined zircon. Details of raw data are summarized in Tables S2 and S3*

| Sample | ID | $^{238}U/^{206}Pb^*$ | err (abs) | $^{204}Pb/^{206}Pb^*$ | err (abs) | $^{207}Pb/^{206}Pb^*$ | err (abs) |
|---|---|---|---|---|---|---|---|
| zircon1 | 1.1 | 1.308 | 0.035 | 1.101E-04 | 1.728E-05 | 3.432E-01 | 3.063E-03 |
| zircon2 | 2 | 1.324 | 0.037 | 1.060E-04 | 9.052E-06 | 3.256E-01 | 1.066E-03 |
| zircon3 | 3.1 | 1.417 | 0.037 | 2.222E-04 | 1.771E-05 | 3.312E-01 | 1.151E-03 |
| zircon4 | 4.1 | 1.340 | 0.043 | 8.189E-05 | 7.992E-06 | 3.369E-01 | 8.064E-04 |
| zircon5 | 5.1 | 1.327 | 0.039 | 1.033E-04 | 1.291E-05 | 3.352E-01 | 7.784E-04 |
| zircon6 | 6 | 1.365 | 0.044 | 1.118E-04 | 8.865E-06 | 3.361E-01 | 9.116E-04 |
| zircon7 | 7.1 | 1.418 | 0.040 | 1.307E-04 | 9.751E-06 | 3.045E-01 | 1.867E-03 |
| zircon8 | 8 | 1.349 | 0.043 | 7.558E-05 | 9.674E-06 | 3.308E-01 | 8.395E-04 |
| zircon9 | 9.1 | 1.320 | 0.038 | 1.296E-04 | 1.100E-05 | 3.384E-01 | 8.388E-04 |
| zircon10 | 10.1 | 1.309 | 0.036 | 1.584E-04 | 1.821E-05 | 3.300E-01 | 1.399E-03 |
| | 10.3 | 1.424 | 0.040 | 9.199E-05 | 1.067E-05 | 3.404E-01 | 1.164E-03 |
| | 10.5 | 2.075 | 0.063 | 2.785E-03 | 2.030E-04 | 3.002E-01 | 4.083E-03 |
| | 10.9 | 1.265 | 0.033 | 1.245E-04 | 1.057E-05 | 3.356E-01 | 1.031E-03 |
| zircon11 | 11 | 1.375 | 0.037 | 1.292E-04 | 1.899E-05 | 3.309E-01 | 1.508E-03 |
| zircon12 | 12 | 1.332 | 0.038 | 6.195E-05 | 8.122E-06 | 3.400E-01 | 1.187E-03 |
| zircon13 | 13 | 1.312 | 0.034 | 1.209E-04 | 9.177E-06 | 3.339E-01 | 9.180E-04 |
| zircon14 | 14 | 1.272 | 0.032 | 7.837E-05 | 7.495E-06 | 3.369E-01 | 7.901E-04 |
| zircon15 | 15 | 1.325 | 0.039 | 8.708E-05 | 1.028E-05 | 3.351E-01 | 2.520E-03 |
| zircon16 | 16.2 | 1.270 | 0.033 | 3.905E-05 | 4.750E-06 | 3.382E-01 | 7.544E-04 |
| | 16.3 | 1.252 | 0.033 | 4.925E-05 | 6.046E-06 | 3.291E-01 | 1.347E-03 |

zircon with $\delta$D analysis of the apatite inclusions, the primitive $\delta$D value of the co-existing magma can be estimated. However, determining the $\delta$D value of inclusions has been a challenge due to the small crystal size, often less than 10 $\mu$m in diameter. Koike *et al*. (2016) proposed a new method to measure the D/H ratios of micro-scale apatite grains found in Martian meteorites, using a lateral high-resolution secondary ion mass spectrometry (NanoSIMS50).

In the present study, high spatial resolution D/H ratio analysis, improving upon Koike *et al*. (2016), was applied to zircon-hosted apatite inclusions from the NGB using a NanoSIMS50. U-Pb dating of the host zircon was also carried out to determine the crystallization age of the host rock. This pioneering work has obtained primitive $\delta$D values from micron-scale apatite inclusions, isolated from late isotope fractionation caused by metamorphism or contaminations from modern water, for the first time.

## Materials and Methods

Analyzed zircon crystals, hosting apatite inclusions, were found in tonalite samples collected from the NGB. The sample (POR23; David *et al*., 2009) examined in the present study, was found in the tonalitic unit that formed an outer rim of the NGB. This tonalite consists of fine-grained assemblage of plagioclase, quartz, and biotite with minor zircon grains (O'Neil *et al*., 2011). The tonalite age estimated by U-Pb dating of zircon through thermal ionization mass spectrometry (TIMS) measurement is 3661 ± 1.6 Ma (David *et al*., 2009). This tonalite might have been formed by the partial melting of pre-existing lithologies, including a Hadean basaltic precursor and a mafic juvenile crust (O'Neil *et al*., 2012). The average size of zircon crystals found in this tonalite is approximately 100 $\mu$m, with euhedral to subhedral morphology. Apatite inclusions were found in the studied zircon grains (Fig. 1b).

The zircon crystals were physically separated from the tonalite and mounted in epoxy resin together with Quartz-Gabbro-Norite-Gneiss (QGNG) reference zircon grains from Cape Donnington, South Australia (Takahata *et al*., 2008). The surface of the mount was mirror-polished. Out of 200 zircon grains, seven apatite inclusions with euhedral shapes were found. Mineral identification was performed using both an optical microscope and a scanning electron microscope with energy diffraction X-ray spectroscopy (SEM/EDX; Hitachi S-3400N). The surface was gold-coated for both SEM/EDX and NanoSIMS analyses to avoid the electric charge.

### *NanoSIMS analysis*

*U-Pb and Pb-Pb dating of zircon crystals* Secondary ions, $^{30}Si^+$, $^{90}Zr_2{}^{16}O^+$, $^{204}Pb^+$, $^{206}Pb^+$, $^{238}U^{16}O^+$, and $^{238}U^{16}O_2{}^+$, were measured simultaneously using electron multipliers (EM) on a multi-collector system during a $^{238}U$-$^{206}Pb$ dating session analyzing 41 spots on 16 grains. A 5 nA of $O^-$ primary ion beam was used with <15 $\mu$m spot size. The calibration protocols to obtain the true $^{238}U/^{206}Pb$ ratios are described in Takahata *et al*. (2008). After $^{238}U$-$^{206}Pb$ measurements, $^{204}Pb^+$, $^{206}Pb^+$, and $^{207}Pb^+$ were meas-

ured by a single collector in magnetic jumping mode for $^{207}$Pb-$^{206}$Pb dating of the 16 zircon grains. Detailed analytical procedures are described in Takahata *et al*. (2008). The U-Pb age of the QGNG reference zircon was reported to be 1849.8 ± 1.1 Ma, determined through the conventional method (TIMS). U-Pb dating was only performed on zircon crystals, and not on apatite inclusions, because their grain sizes (<15 $\mu$m) were smaller than the spot size. The background noise of detector EM#4, which was used to collect Pb isotopes in both sessions, were monitored during the measurements of $^{207}$Pb-$^{206}$Pb dating session, resulting 0 in the present study.

*Bulk rock D/H ratio measurements* The $\delta$D value of the bulk rock ($\delta D_{bulk}$) was determined for the host tonalite sample. An approximately 10 grams rock chip was used, avoiding the weathering surface. The rock chip was ultrasonically cleaned in ultrapure water and ethanol to remove superficial contamination. The rock chip was then ground to a powder using an agate mortar down to approximately 10 $\mu$m of grain size. The hydrogen isotope measurement was performed using a PICARRO L2120-i at the Atmosphere and Ocean Research Institute of the University of Tokyo. Approximately 1 gram of powdered sample was loaded into a gas extraction line and pre-vacuumed over night at 100°C to remove the surface-adsorbed water (Gong *et al*., 2007). The sample was then combusted in the oxygen atmosphere at 1200°C for 1 hour. Finally, 14 milligrams of water were extracted and trapped in the finger trap. Approximately 2.5 $\mu$L of water was used per isotope measurement by the PICARRO L2120-i. The analytical uncertainty of the $\delta D_{bulk}$ value was determined through repeat analyses of sample water ($n$ = 4) and the typical repeat measurement of three reference water samples (SLW2, DOW, and ICE2 from SI science Co., Ltd.).

*D/H ratio measurements of apatite inclusion crystals* The D/H ratio measurement protocol was based on that of Koike *et al*. (2016). A $Cs^+$ ion with a 200 pA intensity and a spot diameter of approximately 1 $\mu$m was used as the primary ion beam. Both $^1H^-$ and $^2H^-$ ions were measured by two electron multipliers (EM#3 and #5) simultaneously, using a multi-collection system for 3000 seconds (30 seconds × 100 cycles). The $^{18}O^-$ ion was measured separately following hydrogen analysis on the same spots for 300 seconds (30 seconds × 10 cycles) using a different EM (EM#4), because the secondary ion trajectory and the intensity were substantially different between hydrogen and oxygen. An electron gun (eGun) was used to compensate for electronic charging by the primary ion beam on the sample surface. To reduce contamination from the surface surrounding the analyzed area, pre-sputtering and beam blanking were adopted. For pre-sputtering, a 200 pA primary ion beam was scanned over a 10 × 10 $\mu m^2$ area for 300 seconds. After pre-sputtering, only the inner approximately 2.5 × 2.5 $\mu m^2$ area of the initial area was scanned and measured, meaning that only 6.25% of the total secondary ions produced were collected. This was also effective to reduce the background noise of detectors.

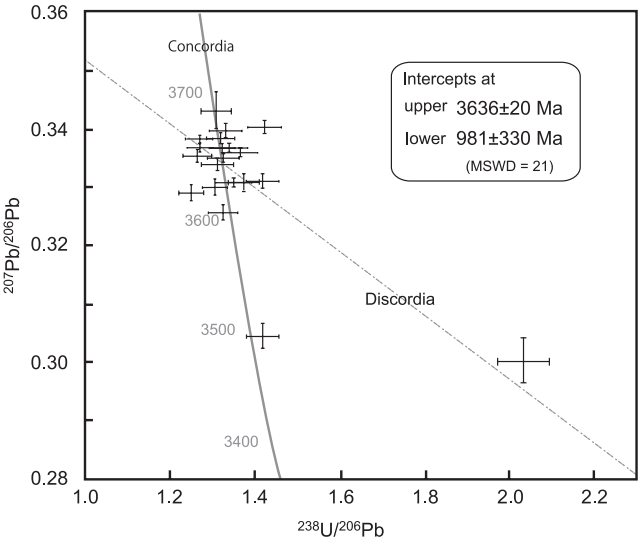


*Fig. 2. Terra-Wasserburg Concordia of sample zircons. Cross marks indicate calculated data of samples and their analytical errors in 1 standard deviation. Solid and dashed lines indicate concordant and discordant lines, respectively. Numbers on solid line indicate Concordia ages in Ma unit. All data were calculated using Isoplot software (Ludwig, 2003).*

## Results and Discussion

*U-Pb dating of zircon crystals*

The U-Pb results were summarized in Table 1. The measured total counts of each secondary ion, $^{30}Si^+$, $^{90}Zr_2{}^{16}O^+$, $^{204}Pb^+$, $^{206}Pb^+$, $^{238}U^{16}O^+$, and $^{238}U^{16}O_2{}^+$, and calculated ratios of $^{204}Pb^+/^{206}Pb^+$, $^{206}Pb^+/^{238}U^{16}O^+$, $^{238}U^{16}O_2{}^+/^{238}U^{16}O^+$, and $^{238}U^{16}O^+/^{96}Zr_2{}^{16}O^+$ of the reference zircon (QGNG) and those of the samples were summarized in Supplementary Tables S1 and S2 respectively. The calibration line for $^{238}$U-$^{206}$Pb age and its original data set were summarized in Supplementary Fig. S1 and Table S1 in the supplementary information. The $^{238}U/^{206}Pb$ ratios of samples were calculated using this calibration line. Detailed procedure was described in elsewhere (Takahata *et al*., 2008). Mean count rates for secondary ions of examined samples were $2.82 \times 10^5$ count per second for 1 nA (cps/nA) for $^{30}Si^+$, $1.88 \times 10^3$ cps/nA for $^{90}Zr_2{}^{16}O^+$, $3.23 \times 10^{-2}$ cps/nA for $^{204}Pb^+$, $2.85 \times 10^2$ cps/nA for $^{206}Pb^+$, $1.15 \times 10^3$ cps/nA for $^{238}U^{16}O^+$, and $3.89 \times 10^2$ cps/nA for $^{238}U^{16}O_2{}^+$, respectively. Calculated $^{238}U/^{206}Pb$ ratios and estimated $^{238}$U-$^{206}$Pb ages of the samples were also summarized in Table S2. The mean $^{238}$U-$^{206}$Pb age of the samples is 3537 ± 76 Ma ($n$ = 41). The total

*Table 2. Results of $^{2}H^{-}/^{1}H^{-}$ and $^{18}O^{-}/^{1}H^{-}$ ratios, total counts of $^{1}H^{-}$, $^{2}H^{-}$, and $^{18}O^{-}$ of measured reference and sample apatite. δD values were calculated after IMF correction.*

| Sample | | $^{2}H^{-}/H^{-}$ | err (abs) | $^{18}O^{-}/H^{-}$ | err (abs) | Total $H^{-}$ | Total $^{2}H^{-}$ | Total $^{18}O^{-}$ | $\delta D_{SMOW}$ (‰)* | err (abs) | OH (wt%) |
|---|---|---|---|---|---|---|---|---|---|---|---|
| Morocco | m1 | 1.36E-04 | 9.12E-06 | 4.7 | 0.01 | 1.52E+06 | 207 | 7.15E+05 | –91 | 59 | 0.79 |
| | m2 | 1.32E-04 | 1.01E-05 | 4.7 | 0.01 | 1.41E+06 | 185 | 6.60E+05 | –118 | 65 | 0.79 |
| | m3 | 1.45E-04 | 9.73E-06 | 4.5 | 0.01 | 1.38E+06 | 200 | 6.18E+05 | –31 | 62 | 0.79 |
| | average | 1.37E-04 | | | | | | | –80 | | |
| | stdev | 6.64E-06 | | | | | | | 45 | | |
| Russia | r1 | 1.35E-04 | 1.59E-05 | 14.4 | 0.03 | 5.19E+05 | 70 | 7.46E+05 | –97 | 102 | — |
| | r2 | 1.36E-04 | 1.64E-05 | 12.7 | 0.02 | 5.45E+05 | 74 | 6.92E+05 | –90 | 106 | — |
| | r3 | 1.35E-04 | 1.57E-05 | 13.3 | 0.02 | 5.63E+05 | 76 | 7.47E+05 | –95 | 101 | — |
| | average | 1.35E-04 | 1.60E-05 | | | | | | –94 | | |
| | stdev | 5.48E-07 | | | | | | | 4 | | |
| Apatite inclusion | apt1 | 1.53E-04 | 1.09E-05 | 5.9 | 0.01 | 1.11E+06 | 169 | 6.56E+05 | 22 | 70 | 0.62 |
| | apt2 | 1.28E-04 | 1.68E-05 | 36.7 | 0.04 | 5.14E+05 | 66 | 2.27E+06 | –140 | 108 | 0.12 |
| | apt3 | 1.20E-04 | 1.45E-05 | 18.2 | 0.03 | 6.09E+05 | 73 | 1.11E+06 | –197 | 93 | 0.20 |
| | apt4 | 1.17E-04 | 2.03E-05 | 41.2 | 0.06 | 3.23E+05 | 38 | 1.60E+06 | –213 | 130 | 0.11 |
| | apt5 | 1.59E-04 | 1.49E-05 | 5.2 | 0.01 | 7.99E+05 | 127 | 4.14E+05 | 65 | 96 | 0.70 |
| | apt6 | 1.52E-04 | 2.30E-05 | 24.2 | 0.04 | 2.82E+05 | 43 | 8.20E+05 | 20 | 148 | 0.18 |
| | apt7 | 1.16E-04 | 2.57E-05 | 51.0 | 0.10 | 2.25E+05 | 26 | 1.25E+06 | –225 | 181 | 0.08 |
| Zircon | | 7.40E-05 | 3.37E-05 | 218 | | 6.76E+04 | 5 | 1.48E+06 | –504 | 217 | |
| Holder | | 1.18E-04 | 8.36E-05 | — | — | 1.70E+04 | 2 | — | –211 | 537 | |

**Calculated after IMF correction. Standard D/H ratio of SMOW = $1.5576e^{-4}$ was used.*
*$^{18}O^{-}/H^{-}$ ratios were calculated considering the differences of accumulation time.*

counts of secondary ions, calculated $^{204}Pb/^{206}Pb$ and $^{207}Pb/^{206}Pb$ ratios, and estimated $^{207}Pb$-$^{206}Pb$ ages in the Pb-Pb session, were summarized in Supplementary Table S3. The mean count rates for secondary ions of $^{204}Pb^+$, $^{206}Pb^+$, and $^{207}Pb^+$ of examined samples were $4.34 \times 10^{-2}$, $2.75 \times 10^2$ and $9.15 \times 10^1$ cps/nA, respectively. The average $^{207}Pb$-$^{206}Pb$ age is 3624 ± 7 Ma.

Figure 2 shows the Tera-Wasserburg Concordia diagram for 20 analytical spots. The $^{207}Pb$-$^{206}Pb$ dating was performed on one to three of the same spots for which $^{238}U$-$^{206}Pb$ dating was performed, to examine the concordance of each age. 19 of these coincide with the Concordia line. One point, which was obtained from the rim of zircon grain #10, plotted off the Concordia line, suggesting lead loss during later metamorphic episodes (David *et al*., 2009). The estimated Concordia age found in this study is 3636 ± 20 Ma, which is within the analytical uncertainty of the previous TIMS-determined age for the same tonalite (3661.1 ± 4.1 Ma; David *et al*., 2009). Considering the euhedral occurrences of the apatite inclusions, it is inferred that their crystallization age is slightly older than that of host zircon. We therefore assume that the age of examined apatite inclusions is at least 3.64 Ga.

*D/H ratios of apatite*

$^2H^-/^1H^-$ and $^{18}O^-/^1H^-$ ratios were calculated from the measured total ion counts of $^1H^-$, $^2H^-$, and $^{18}O^-$ for both reference and sample apatite grains. These results are summarized in Table 2. The average count rates of $^1H^-$ and $^2H^-$ of seven apatite inclusions were 184 cps and 0.03 cps, respectively. The cycle by cycle trend of hydrogen isotope analysis was monitored and suggested that there was no apparent contamination which has a different hydrogen isotope values, such as cracks or tiny melt inclusions, during measurements (Supplementary Fig. S2).

The background noise during hydrogen isotope analysis was examined by several approaches in the present study. In our analytical procedure, the background noise for each detector cannot be excluded during the hydrogen isotope measurement. We performed several measurements to know the background noise of analysis as follows: 1) the background noise on detectors of EM#3 and #5 were monitored during the $^{18}O^-$ measurement which detected by EM#4. The mass numbers applied for EM#3 and #5 were 14.6 and 29.2, respectively. The total counts of them were 0 during 300 seconds of $^{18}O^-$ analysis on reference apatite and sample apatite, suggesting that the background noise of detectors EM#3 and #5 were less than 1 count (0.004 cps). 2) We measured the background noise in the same analytical conditions with hydrogen isotope measurement in the separated session as follows: a) count $^1H^-$ and $^2H^-$ ion counts on the reference apatite (Morocco apatite) without turning on the primary ion beam, b) measure $^1H^-$ and $^2H^-$ ions on the Morocco apatite without turning on the high voltage of secondary ion extraction lens. In case a), we can estimate the background noise generated from apatite itself. The $^1H^-$ and $^2H^-$ ion counts were manually counted in the same analytical condition with hydrogen isotope measurement, but without shooting the primary ion beam on the sample surface. As a result of monitoring and manual counting for 300 seconds, count rates of $^1H^-$ and $^2H^-$ were 30 ± 5.5 (1 standard deviation: 1SD) cps and less than 0.004 cps, respectively. In case b), we could estimate the background noise of EM#3 and #5 in the same condition with hydrogen isotope measurement, but without turning on the secondary ion extraction lens. Measured count rates for EM#3 and #5 were 33 ± 5.7 (1SD) cps and less than 0.0004 cps, respectively. In addition, count rates of $^1H^-$ and $^2H^-$ on the sample holder and zircon were measured in the same analytical condition with hydrogen isotope measurement, resulting 14 ± 12 cps and 0.001 ± 0.001 cps, respectively (Table 2). We concluded that these values, measured on the sample holder and zircon, were composed of the mixture of the background noise of detectors and contamination from the analytical atmosphere, and were the maximum values for the background noise of this analysis. The effect of these background noise on this analysis was validated in the following section.

The instrumental mass fractionation (IMF) factor for D/H ratios was determined using an internal reference material (Morocco apatite) with a known D/H ratio and OH concentration (D/H = $1.43 \times 10^{-4}$, OH = 0.79 ± 0.16%, Barnes *et al*., 2013; Koike *et al*., 2016). The IMF correction factor (f) is calculated as:

$$(D/H)_{ref,\ true} = f \times (^2H^-/^1H^-)_{ref,\ meas.} \quad (1)$$

where $(D/H)_{ref,\ true}$ and $(^2H^-/^1H^-)_{ref,\ meas.}$ indicate the true D/H ratio and the measured $^2H^-/^1H^-$ ratios of the reference material respectively. The average $^2H^-/^1H^-$ ratio of the Morocco apatite was $(1.37 \pm 0.10) \times 10^{-4}$, corresponding to an "f" value of 1.04 ± 0.07 (1SD). This value is consistent with our previous study, within analytical uncertainty (Koike *et al*., 2016). The "Russia" apatite was also used as a second reference material for the analysis, and its D/H ratio and OH concentration were determined through the same combustion method as for the Morocco apatite (D/H = $1.40 \times 10^{-4}$ and OH = 0.30%). The average $^2H^-/^1H^-$ ratios of the Russia apatite is $1.35 \pm 0.16 \times 10^{-4}$. Its calculated IMF-corrected $(D/H)_{ref,\ true}$ ratio was $1.41 \pm 0.17 \times 10^{-4}$, indicating that these values are the same as the true value, within 1 (1SD) of analytical uncertainty.

The $\delta D$ values of seven apatite inclusions were calculated using "f" and measured $^2H^-/^1H^-$ ratios (Table 2). Figure 3 shows the correlation between $\delta D$ values and $^{18}O^-/^1H^-$ ratios of the examined apatite inclusions. Large

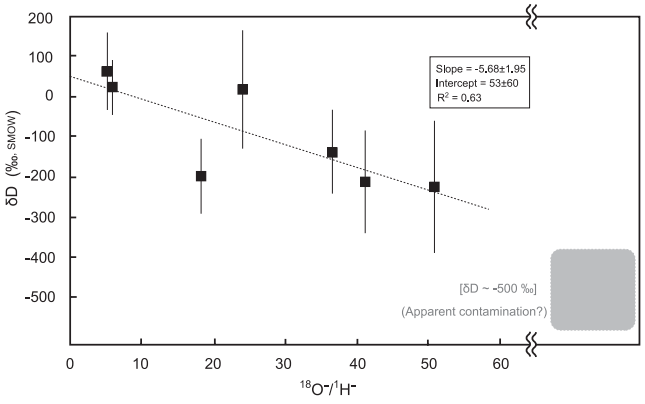


*Fig. 3. Correlation diagram of $^{18}O^-/H^-$ ratio vs. δD values of examined 7 apatite inclusions. Error bars on each data point indicate 1sigma of analytical error. A negative trend was observed (dashed line). Slope and intercept are calculated to be –5.68 ± 1.95 and 52.8 ± 59.8, respectively. Gray square indicates the apparent contamination values.*

variation exists in both δD values and $^{18}O^-/^1H^-$ ratios. A negative correlation between δD values and $^{18}O^-/^1H^-$ ratios was observed, with a slope and intercept of –5.68 ± 1.95 and 52.8 ± 59.9 respectively. Generally, the higher the $^{18}O^-/^1H^-$ ratio, the lower the δD value, with increasing analytical uncertainty in this direction as well. This trend suggests mixing between the pristine δD value, characterized by a lower $^{18}O^-/^1H^-$ ratio and a very low δD value that could be derived from contamination, including the background noise of hydrogen isotope analysis. The δD value and $^{18}O^-/^1H^-$ ratio of the host zircon grain were found to be δD = –504 ± 220‰ and O/H = 218. The low $^1H^-$ ion counts and δD value of the zircon were similar to those determined for the metal sample holder of the NanoSIMS50 (Table 2), suggesting that the contaminated component has very low δD value, of approximately –500‰. We therefore interpreted this negative trend as resulting from the mixing of the pristine δD value of the apatite inclusions with a H-rich contamination component in the analytical atmosphere of the NanoSIMS50.

Supplementary Fig. S3 demonstrates that the apparent mixing between pristine hydrogen from apatite inclusions and contamination hydrogen which was assumed to have δD = –500‰. This can be described by the following equations:

$$\delta D_M = f_S \times \delta D_S + f_C \times \delta D_C \quad (2)$$

$$(O/H)_M = f_S \times (O/H)_S + f_C \times (O/H)_C \quad (3)$$

$$f_S + f_C = 1 \quad (4)$$

$$f_S = 1/(1 + k \times (O/H)_S) \quad (5)$$

where subscripts M, S, and C refer to the measured value, sample pristine component, and contaminated component respectively. The "k" is a constant, determined by the ratio of the $^1H^-$ intensity of sample to that of contamination. We assumed $\delta D_C$ = –500‰ based on the δD values determined for the zircon and the sample holder. To explain the negative trend observed in Fig. 3, a constant contamination $^1H^-$ ion signal intensity (of approximately 600 cps) was assumed, and the varying $^1H^-$ ion intensity of the apatite inclusions ($10^3$ to $10^5$ cps) was estimated. The pristine δD of apatite inclusions was therefore uniquely determined to be 52.8 ± 59.9‰. As this pristine δD value is the intercept of the mixing trend of measured δD values, it could be determined independently to δD value and $^1H^-$ ion intensity of the H-rich contamination component (Supplementary Fig. S4).

Metamorphic hydrogen isotope fractionation in apatite inclusions is likely not the cause of this negative trend in the present study (Fig. 3). In such a case, it is expected that $^1H$ would be lost faster than D during fractionation, resulting in D-rich and H-depleted apatite, which is the opposite of what is observed in Fig. 3.

Through repeat analyses of water extracted from the bulk tonalite ($n$ = 4), the $\delta D_{bulk}$ value was determined to be –49.2 ± 4.2‰. This negative value is consistent with the δD of Archean age serpentine (Pope *et al*., 2012, and references therein). The major host of hydrogen in the bulk sample would be biotite with minor contribution of possible OH-bearing phases in the grain boundaries which have been suffered a metamorphism. Thus the $\delta D_{bulk}$ value would be a mixture of ambiguous origin of hydrogen.

The δD value of the apatite inclusions determined in the present study, +52.8 ± 59.9‰, is quite different from such bulk rock values. This indicates that the hydrogen in the apatite inclusions hosted in zircon crystals have been isolated from the structural water, such as OH in biotite and grain boundaries, in the tonalite. This further suggests that the pristine δD value of water in the source magma may have been preserved in these zircon-protected apatite inclusions.

*Geochemical implications*

The positive δD value for tonalite source magmas of the NGB (52.8 ± 59.9‰) suggests that the hydrogen (water) in the tonalitic magma chamber was depleted in $^1H$ at 3.64 Ga ago. The δD value of the tonalitic magma chamber may be a proxy for the δD value of the global ocean. Geological studies of this area suggest that the examined tonalite was formed through the partial melting of the mafic crust (O'Neil *et al*., 2008, 2012; Turner *et al*., 2014). The driving force behind the partial melting of the crust is still debated, however, two tectonic settings have been invoked.

One is a model of subduction and addition of water

by the dehydration of the oceanic crust (Drummond and Defant, 1990; Turner *et al*., 2014). In this scenario, the water in the tonalite source magma originated from water dehydrated from the subducting oceanic crust in the Archean era. Hydrogen in the tonalitic magma chamber would have been incorporated into the apatite during its crystallization, which are finally captured in the zircon crystals in the early stage of the tonalite formation. The $\delta$D value of the Archean ocean may be further constrained by the $\delta$D value of magmatic water. In a modern subduction setting, an isotopic shift of approximately 16‰ is expected in hydrogen between the subducting slab and dehydrating fluid (Shaw *et al*., 2008). The preferential release of D-rich fluids from a subducting slab was experimentally proposed in previous studies (Sakai and Tsutsumi, 1978; Vennemann and O'Neil, 1996). Such isotope fractionation was consistent with the observed $\delta$D values between a subducting slab ($\delta$D = –87 to –50‰), and melt inclusions in the Mariana Trough in the modern environment ($\delta$D = –34 ± 13‰) (Clog *et al*., 2013; Shaw *et al*., 2008). Assuming the same isotopic shift in the present study, an original oceanic crust of $\delta$D = +37 ± 60‰ is calculated at that age. The hydrogen isotope fractionation between ocean water and oceanic crust was estimated to be –50‰ based on the serpentinized peridotite (Agrinier *et al*., 1995; Margaritz and Taylor, 1976; Pope *et al*., 2012). Finally, the $\delta$D value of the Archean ocean can be estimated to be +87 ± 60‰. Even if the lowest $\delta$D value for the Archean ocean is taken, +27‰, it is significantly heavier than that of estimated for the Archean ocean based on the $\delta$D measurements of serpentine of the same age (–25 ± 5‰: Pope *et al*., 2012).

The other possibility is that the tonalite formed through the melting of thickened mafic oceanic crust (e.g., Nutman *et al*., 1999; Smithies, 2000; Condie, 2005; Nagel *et al*., 2012). This model does not necessarily require a subduction setting for the partial melting of the crust, while the pressure of 10 to 14 kbar, which corresponds to the thickness of crust between 35 and 50 km, is necessary under Archean geothermal condition (Smithies, 2000; Nagel *et al*., 2012). In this case, water in the tonalitic magma chamber was originated from the oceanic crust itself. Approximately 50‰ of difference between ocean water and oceanic crust is proposed for the $\delta$D values (e.g., Shaw *et al*., 2008; Pope *et al*., 2012), suggesting that the $\delta$D value of Archean ocean can be 50‰ heavier than that of oceanic crust and the tonalitic magma, up to 103‰, in the present study.

In calculations and estimates made in the present study, specific isotope fractionation caused by particular geological processes and mineralization were assumed to be the same as those of modern phenomena, such as: hydrothermal reaction between ocean water and oceanic crust, slab dehydration during subduction, partial melting and magma production, and hydrogen diffusion into mineralized apatite from the magma chamber. These isotope fractionation mechanisms are sensitive to the temperature and chemical composition of the ocean, oceanic crust and mantle compositions, dehydration rates during subduction, and geothermal gradient of the interior Earth in the Archean era. Such factors are expected to cause the magnitude of the hydrogen isotope shift to be greater than the analytical uncertainty of the present study.

## Conclusions

The $\delta$D values of micro-scale apatite inclusions, enclosed in zircon crystals from a tonalite of the NGB, were successfully determined together with U-Pb dating of the host zircon using a NanoSIMS50. The U-Pb crystallization age of the examined zircon grains was 3636 ± 20 Ma. The protolith age is consistent with the age previously reported for the same tonalitic unit (David *et al*., 2009). The pristine $\delta$D value of apatite inclusions was determined from values measured in seven apatite inclusions to be +53 ± 60‰, corresponding to the tonalitic source magma. Using a simple water-rock interaction model, the corresponding $\delta$D value of the Archean ocean would be at least +27‰. The $\delta$D value of the Archean ocean estimated here is heavier than that previously proposed (Pope *et al*., 2012). Further studies on the Archean rock record are called for to univocally constrain the primitive oceanic isotopic composition and its extraterrestrial sources.

**Acknowledgments**—We are greatful to Toshihiro Miyajima for his technical support of PICARRO L2120-i. We appreciate two reviewers for their constructive comments. We also appreciate, Dr. Hisayoshi Yurimoto, as an associate editor, for his incisive and valuable comments. This research was supported by KAKENHI (24221002) for Y.S. and N.T. (26106005). Computer software "Isoplot/Ex" was kindly provided by Dr. K. R. Ludwig.

## References

Agrinier, P., Hekinian, R., Bideau, D. and Javoy, M. (1995) O and H stable isotope compositions of oceanic crust and upper mantle rocks exposed in the Hess Deep near the Galapagos Triple Junction. *Earth Planet. Sci. Lett.* **136**, 183–196.

Allard, P. (1983) The origin of hydrogen, carbon, sulphur, nitrogen and rare gases in volcanic exhalations: evidence from isotope geochemistry. *Forecasting Volcanic Events* (Tazieff J. and Sabroux C., eds.), 337–386, Elsevier, Amsterdam.

Andreasen, R. and Sharma, M. (2009) Comment on "Neodymium-142 Evidence for Hadean Mafic Crust". *Science* **325**, 267.

Arai, T., Omori, S., Komiya, T. and Maruyama, S. (2015) Intermediate P/T-type regional metamorphism of the Isua

Supracrustal Belt, southern west Greenland: The oldest Pacific-type orogenic belt? *Tectonophysics* **662**, 22–39.

Barnes, J. J., Franchi, I. A., Anand, M., Tartèse, R., Starkey, N. A., Koike, M., Sano, Y. and Russell, S. S. (2013) Accurate and precise measurements of the D/H ratio and hydroxyl content in lunar apatites using NanoSIMS. *Chem. Geol.* **337–338**, 48–55.

Cates, N. L. and Mojzsis, S. J. (2007) Pre-3750 Ma Supracrustal rocks from the Nuvvuagittuq Supracrustal belt, northern Quebec. *Earth Planet. Sci. Lett.*, **255**, 9–21.

Cawood, P. A., Hawkesworth, C. J. and Dhuime, B. (2013) The continental record and the generation of continental crust. *Geol. Soc. Am. Bull.* **125**, 14–32.

Clog, M., Aubaud, C., Cartigny, P. and Dosso, L. (2013) The hydrogen isotopic composition and water content of southern Pacific MORB: A reassessment of the D/H ratio of the depleted mantle reservoir. *Earth Planet. Sci. Lett.* **381**, 156–165.

Condie, K. C. (2005) TTGs and adakites: Are they both slab melts? *Lithos* **80**, 33–44.

David, J., Godin, L., Stevenson, R., O'Neil, J. and Francis, D. (2009) U-Pb ages (3.8–2.7 Ga) and Nd isotope data from the newly identified Eoarchean Nuvvuagittuq supracrustal belt, Superior Craton, Canada. *Geol. Soc. Am. Bull.* **121**, 150–163.

Dhuime, B., Hawkesworth, C. J., Cawood, P. A. and Storey, C. D. (2012) A change in the geodynamics of continental growth 3 billion years ago. *Science* **335**, 1334–1336.

Drummond, M. S. and Defant, M. J. (1990) A model for trondhjemite-tonalite-dacite genesis and crustal growth via slab melting: Archean to modern comparisons. *J. Geophys. Res.* **95**, 21503–21521.

Furnes, H., Wit, M., Staudigel, H., Rosing, M. and Muehlenbachs, K. (2007) A vestige of Earth's oldest ophiolite. *Science* **315**, 1704–1707.

Giggenbach, W. F. (1992) Isotopic shifts in waters from geothermal and volcanic systems along convergent plate boundaries and their origin. *Earth Planet. Sci. Lett.* **113**, 495–510.

Gong, B., Zheng, Y. and Chen, R. (2007) TC/EA-MS online determination of hydrogen isotope composition and water concentration in eclogitic garnet. *Phys. Chem. Min.* **34**, 687–698.

Griffin, W. L., Belousova, E. A., Shee, S. R., Pearson, N. J. and O'Reilly, S. Y. (2004) Archaean crustal evolution in the northern Yilgarn Craton. U-Pb and Hf-isotope evidence from detrital zircons. *Precam. Res.* **131**, 231–282.

Jenner, F. E., Bennett, V. C., Nutman, A. P., Friend, C. R. L., Norman, M. D. and Yaxley, G. (2009) Evidence for subduction at 3.8 Ga: Geochemistry of arc-like metabasalts from the southern edge of the Isua Supracrustal Belt. *Chem. Geol.* **261**, 83–98.

Koike, M., Sano, Y., Takahata, N., Ishida, A., Sugiura, N. and Anand, M. (2016) Combined investigation of H isotopic compositions and U-Pb chronology of young Martian meteorite Larkman Nunatak 06319. *Geochem. J.* **50**, 363–377.

Komiya, T., Yamamoto, S., Aoki, S., Sawaki, Y., Ishikawa, A., Tashiro, T., Koshida, K., Shimojo, M., Aoki, K. and Collerson, K. D. (2015) Geology of the Eoarchean, >3.95 Ga, Nulliak supracrustal rocks in the Saglek Block, northern Labrador, Canada: The oldest geologic evidence for plate tectonics. *Tectonophysics* **662**, 40–66.

Ludwig, K. R. (2003) User's Manual for Isoplot 3.00: A geochronological toolkit for Microsoft Excel. Special publication/Berkeley Geochronology Center No. 4, 74 pp.

Margaritz, M. and Taylor, H. P. (1976) Oxygen, hydrogen and carbon isotopes studies of Franciscan Formation, Coast Range, California. *Geochim. Cosmochim. Acta* **40**, 215–237.

Miyagi, I. and Matsubaya, O. (2003) Hydrogen isotopic composition of hornblende and biotite phenocrysts from Japanese Island arc volcanoes; evaluation of alteration process of the hydrogen isotopic ratios by degassing and re-equilibration. *J. Volcanol. Geotherm. Res.* **126**, 157–168.

Nagel, T. J., Hoffmann, J. E. and Munker, C. (2012) Generation of Eoarchean tonalite-trondhjemite-granodiorite series from thickened mafic arc crust. *Geol. Soc. Am.* **40**(4), 375–378.

Nutman, A. P., Mojzsis, S. J. and Friend, C. R. L. (1997) Recognition of >3850 Ma water-lain sediments in West Greenland and their significance for the early Archean Earth. *Geochim. Cosmochim. Acta* **61**, 2475–2484.

Nutman, A. P., Bennett, V. C., Friend, C. R. L. and Norman, M. D. (1999) Metaigneous (non-gneissic) tonalites and quartz-diorites from an extensive *ca.* 3800 Ma terrain south of the Isua supracrustal belt, southern West Greenland: Constraints on early crust formation. *Contrib. Mineral. Petrol.* **137**, 364–388.

O'Neil, J., Carlson, R. W., Francis, D. and Stevenson, R. K. (2008) Neodymium-142 evidence for Hadean mafic crust. *Science* **321**, 1828–1831.

O'Neil, J., Francis, D. and Carlson, R. W. (2011) Implication of the Nuvvuagittuq Greenstone Belt for the Formation of Earth's Early Crust. *J. Petrol.* **52**, 985–1009.

O'Neil, J., Carlson, R. W., Paquette, J. L. and Francis, D. (2012) Formation age and metamorphic history of the Nuvvuagittuq Greenstone Belt. *Precam. Res.* **220–221**, 23–44.

Patchett, P. J., Kouvo, O., Hedge, C. E. and Tatsumoto, M. (1981) Evolution of continental crust and mantle heterogeneity: evidence from Hf isotopes. *Contrib. Mineral. Petrol.* **78**, 279–297.

Percival, J. A., Mortensen, J. K., Stern, R. A., Card, J. D. and Begin, N. J. (1992) Giant granulite terranes of north- eastern Superior Province; the Ashuanipi Complex and Minto Block. *Can. J. Earth Sci.* **29**, 2287–2308.

Polat, A., Hofmann, A. W. and Rosing, M. T. (2002) Boninite-like volcanic rocks in the 3.7–3.8 Ga Isua greenstone belt, West Greenland: Geochemical evidence for intra-oceanic subduction zone processes in the early Earth. *Chem. Geol.* **184**, 231–254.

Pope, E. C., Bird, D. K. and Rosing, M. T. (2012) Isotope composition and volume of Earth's early oceans. *Proc. Nat. Acad. Sci. USA* **109**, 4371–4376.

Prowatke, S. and Klemme, S. (2006) Trace element partitioning between apatite and silicate melts. *Geochim. Cosmochim. Acta* **70**, 4513–4527.

Sakai, H. and Tsutsumi, M. (1978) D/H fractionation factors between serpentine and water at 100° to 500°C and 2000 bar water pressure, and the D/H ratios of natural serpentines.

*Earth Planet. Sci. Lett.* **40**, 231–242.
Shaw, A. M., Hauri, E. H., Fischer, T. R., Hilton, D. R. and Kelley, K. A. (2008) Hydrogen isotopes in Mariana arc melt inclusions: Implications for subduction dehydration and the deep-Earth water cycle. *Earth Planet. Sci. Lett.* **275**, 138–145.
Smithies, R. H. (2000) The Archaean tonalite- trondhjemite-granodiorite (TTG) series is not an analogue of Cenozoic adakite. *Earth Planet. Sci. Lett.* **182**, 115–125.
Stern, R. J. (2005) Evidence from ophiolites, blue- schists, and ultrahigh pressure metamorphic terranes that the modern episode of subduction tectonics began in Neoproterozoic time. *Geology* **33**, 557–560.
Stern, R. J., Fouch, M. J. and Klempere, S. L. (2003) An overview of the Izu-Bonin-Mariana subduction factory. *Inside the Subduction Factory* (Eiler, J., ed.), AGU Geophysical Monograph 38, 175–222, Washington, D.C.
Stolper, E. and Newman, S. (1994) The role of water in the petrogenesis of Mariana Trough magmas. *Earth Planet. Sci. Lett.* **121**, 293–325.
Takahata, N., Tsutsumi, Y. and Sano, Y. (2008) Ion microprobe U-Pb dating of zircon with a 15-micrometer spatial resolution using NanoSIMS. *Gondwana Res.* **14**, 587–596.
Tang, M., Chen, K. and Rudnick, R. L. (2016) Archean upper crust transition from mafic to felsic marks the onset of plate tectonics. *Science* **351**, 372–375.
Turner, S., Rushmer, T., Reagan, M. and Moyen, J. F. (2014) Heading down early on? Start of subduction on Earth. *Geology* **42**, 139–142.
Vennemann, W. T. and O'Neil, J. R. (1996) Hydrogen isotope exchange reactions between hydrous minerals and molecular hydrogen: I. A new approach for the determination of hydrogen isotope fractionation at moderate temperatures. *Geochim. Cosmochim. Acta* **60**, 2437–2451.
Wallace, P. J. (2005) Volatiles in subduction zone magmas: Concentrations and fluxes based on melt inclusion and volatile gas data. *J. Volcanol. Geotherm. Res.* **140**, 217–240.
Watson, E. B. (1979) Apatite saturation in basic to intermediate magmas. *Geophys. Res. Lett.* **6**, 937–940.
Watson, E. B. (1980) Apatite and phosphorus in mantle source regions: an experimental study of apatite/melt equilibria at pressures to 25 kbar. *Earth Planet. Sci. Lett.* **51**, 322–335.
Yuan, H. (2015) Secular change in Archaean crust formation recorded in Western Australia. *Nat. Geosci.* **8**, 808–813.

## Supplementary Materials

URL (http://www.terrapub.co.jp/journals/GJ/archives/data/52/MS534.pdf)
Figures S1 to S4
Tables S1 to S5